

# RESISTANCE OF STEEL AND COMPOSITE CONNECTIONS UNDER COMBINED AXIAL FORCE AND BENDING INCLUDING GROUP EFFECTS: ANALYTICAL PROCEDURES AND COMPARISON WITH LABORATORY TESTS

Jean-François Demonceau (corresponding author)  
UEE Research Unit  
University of Liège, Belgium  
E-mail: [jfdemonceau@uliege.be](mailto:jfdemonceau@uliege.be)

Frédéric Cerfontaine  
BEC Cerfontaine Design Office  
Liège Belgium  
E-mail: [f.cerfontaine@becerfontaine.be](mailto:f.cerfontaine@becerfontaine.be)

Jean-Pierre Jaspart  
UEE Research Unit  
University of Liège, Belgium  
E-mail: [jean-pierre.jaspart@uliege.be](mailto:jean-pierre.jaspart@uliege.be)

## ABSTRACT

The paper presents some different developments performed in the last years at the University of Liège. In particular, complete component-based analytical procedures to predict the resistance of steel bolted connections subjected to combined bending moments and axial forces (M-N interaction) are introduced and commented. These analytical procedures consider so-called “group effects” between successive bolt-rows and cover possible ductile or brittle connection responses. Then they are extended to composite steel-concrete connections. In a second part, the analytical predictions are compared to available test data. The correlation between the experimentally measured resistances and those provided by the analytical procedures may be considered as close. Finally, the recommendations in terms of M-N interactions provided by Eurocode 3 are critically analysed.

**Keywords:** *Structural bolted steel and steel-concrete composite connections, resistance, bending moment and axial force interaction, Eurocode 3*

# 1. INTRODUCTION

## 1.1 The component method

The design of steel and composite structural joints is covered by Eurocode 3 [1] and Eurocode 4 [2] respectively. The proposed procedure for the joint characterisation is founded on the component method which allows the evaluation of the main mechanical properties of a joint, i.e. its stiffness, its resistance and the associated failure mode, and which has been widely validated through comparisons to experimental and numerical results.

In the component method, it is considered that a joint is made of a set of elements (called components). The mechanical properties of these components, in terms of stiffness and resistance are estimated through appropriate analytical design models or through experimental tests or numerical simulations; then these component properties are “assembled” to predict the mechanical properties of the full joint.

So the evaluation of the joint properties through the component method implies three successive steps:

- identification of the active joint components;
- characterisation of the mechanical properties of these components;
- “assembly” of the components to derive the global mechanical properties of the joint.

The interested reader will find more information about the component method and its field of application in [3].

In Part 1.8 of Eurocode 3 [1], simple analytical calculation procedures are provided for joints in bending and shear; in particular under bending moments, they allow to derive the design moment resistance and the elastic rotational stiffness (called “initial stiffness”) of steel joints. The procedure is extended in Eurocode 4 [2] to the derivation of the structural properties of joints in composite constructions.

## 1.2 Structural joints subjected to bending moment $M$ and axial force $N$

In most of the cases, beam-to-column joints and beam splices are subjected to axial forces (compression or tension) in addition to bending moments and shear forces. These ones have an influence on the rotational stiffness, moment resistance and rotational capacity of the joints.

The component method may obviously be applied as a general procedure for the derivation of mechanical properties of various joint types and loading situations. The individual response of the different components being not linked to the type of loading applied to the full joint, reference may be directly made to Eurocode 3 Part 1-8 and Eurocode 4 to evaluate their stiffness and their resistance. But an appropriate assembly procedure is required to cover the combined application of moments and axial forces. In fact, one of the main difficulties is linked to the fact that the components activated within the joint will vary according to the values of the applied moments and axial forces. This problem is addressed in the present paper, with a focus on the resistance aspects only. For stiffness aspects, reference can be made to [4].

As an alternative, Part 1.8 of Eurocode 3 proposes another approach in which, first, the influence of the M-N interaction is disregarded as long as the axial force  $N_{Ed}$  applied to the joint is smaller than 5% of the axial design plastic resistance of the connected beam cross-section ( $N_{pl,Rd}$ ):

$$\left| \frac{N_{Ed}}{N_{pl,Rd}} \right| \leq 0,05 \quad (1)$$

It means that, below this limit, it is assumed that the axial forces are not significantly influencing the rotational response of the joints. However, looking to the scientific literature, it appears that this criterion is a fully arbitrary one and is not founded on a scientific background.

The 5% rule covers most of the situations met in rectangular multi-storey building frames, but is usually not satisfied in joints located at the extremities of inclined roof beams in industrial frames, as an example.

If the criterion of Formula 1 is not respected, the Eurocodes recommend to consider a linear interaction between M and N, the lines linking the hogging or sagging bending resistances, computed assuming that no axial loads are applied, to the axial resistances in tension or compression, computed assuming that no bending moments are applied to the joint. The criteria as proposed in the Eurocodes result in a polygonal interaction diagram as illustrated on Figure 1.

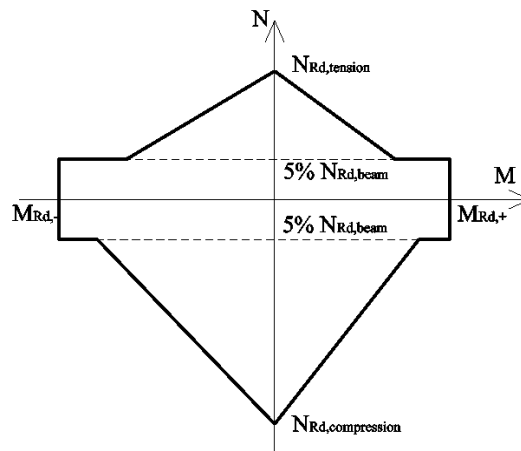


Fig. 1 - M-N resistant interaction curve proposed in Eurocode 3 Part 1-8.

In [4], it has been shown that the Eurocode M-N interaction curve predicts sometimes rather precisely but often very safely the joint resistance, while the 5% rule leads generally to a significant overestimation of the joint resistance. This will be illustrated later on. Besides that, Eurocode 3 Part 1-8 is not defining the way on how to evaluate, through a dedicated assembly procedure, the values of  $N_{Rd,tension}$  and  $N_{Rd,compression}$  reported in Figure 1.

In the present paper, an improved design analytical assembly procedure is presented. It has been first developed and validated by the second author [4] to characterise the properties of ductile and non-ductile steel joints subjected to M-N interaction. It has then been extended to steel-concrete composite joints by the first author [5]. More recently, it has been further

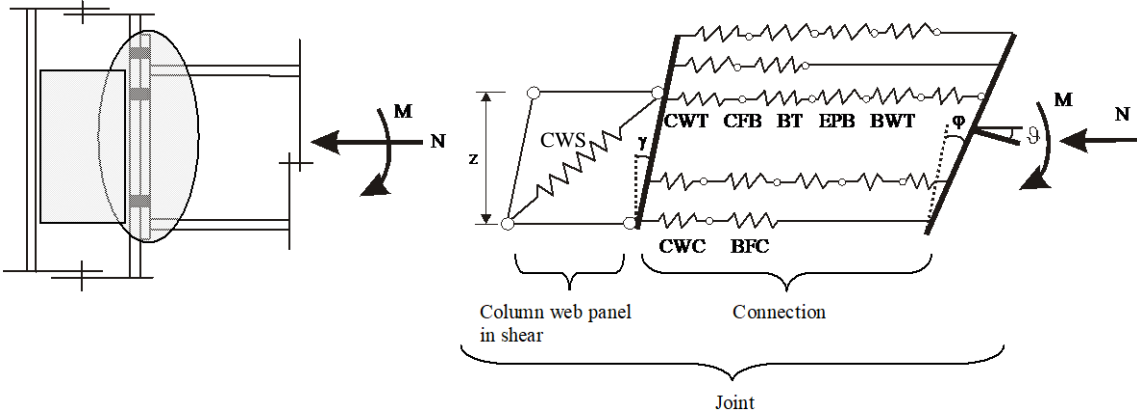
validated through comparisons to more recent results obtained through experimental tests performed on composite beam-to-column joints in various different loading situations, including fire and progressive collapse.

Column bases and column splices transfer also high axial forces in addition to bending moments and therefore do not fulfil the limiting criterion prescribed by Part 1.8. In the latter, a component-based approach for M-N interaction is proposed, for resistance and stiffness evaluation. However, its scope is limited to specific column base configurations.

**2 MECHANICAL MODEL AND PARTICULAR ASPECTS**

The analytical assembly procedure presented below basically refers to the well-known mechanical “spring model” shown on Figure 2 which illustrates the behaviour of a single-sided joint subjected to both bending and axial forces.

In this model, each constitutive component of the joint is illustrated by an extensional spring characterised by a non-linear F-Δ curve, where F and Δ represent respectively the force acting in the component and the related displacement. According to the definitions given in Part 1.8 of Eurocode 3, the joint is seen to be constituted of a *connection* subjected to M and N and a *column web panel* in shear.



Abbreviation	Definition	Abbreviation	Definition
CWT	Column web in tension	BWT	Beam web in tension
CFB	Column flange in bending	CWC	Column web in compression
BT	Bolts in tension	BFC	Beam flange in compression
EPB	End-plate in bending	CWS	Column web in shear

Fig. 2 – Mechanical model classically used in the proposed analytical procedures

In the absence of specific assembly procedure in the Eurocodes for joints under M-N, many authors in the past [6, 7, 8] have “computerised” spring models similar to the one illustrated in Figure 2, i.e. have physically implemented the model and all its constitutive springs in a software, have characterised each component spring by a non-linear F-Δ curve derived through Eurocodes component design rules and have finally increased progressively the M/N loading until a failure is reached in the whole joint, often after internal plastic redistributions amongst the springs, at least the “ductile” ones (components with a significant deformation capacity). In a connection activating “non-ductile” components, the resistance may be limited by one of these components reaching its maximum deformation capacity. In this case, any further plastic redistribution of forces within the connection should be disregarded. The

attainment of the maximum deformation capacity in the “non-ductile” components has therefore to be systematically checked.

This corresponds in fact to a “numerical” assembly approach. However, a numerically complex model does not necessarily yield accurate results when compared with the experiment. This is the case here as, usually, the three following features are generally disregarded in the existing “spring models”:

- *Group effects*: the group effects occur in components made of plates subjected to transverse bolt forces, i.e. mainly the end-plate and column flange in bending components – see respectively EPB and CFB in Figure 2). At the location of the bolts, transverse forces are applied to the plate and a yield plastic mechanism may appear; if the distances between the bolts are significant, separate yield lines will develop in the plate around the bolts (namely “individual bolt mechanism”), while a common yield plastic mechanism around several bolts may occur when the distance between the latter is limited (namely “bolt group mechanism” – see Figure 3). Also, these group effects can affect the behaviour of other components as the column web in tension and the beam web in tension (respectively CWT and BWT in Figure 2).
- *Component interactions*: component interactions may develop in components “extracted” from the column. Indeed, in these components, three types of stresses can interact: longitudinal stresses due to bending moments and axial forces in the column, shear stresses in the column web panel, and transverse stresses associated to the introduction into the column of concentrated compression or tension forces transmitted by the connection(s). Such stresses developed in three following components (Figure 2): column web in tension (CWT), column web in compression (CWC) and column web in shear (CWS). In Eurocode 3 Part 1-8, interaction criteria are provided for the CWT and CWC components while, for the CWS one, a flat rate reduction of 10% is safely recommended (factor 0,9 in the relevant CWS design formula).
- *Height of the column web panel*: the shear force in the column web panel varies along its height, according to the activated connection components, the forces that the latter transfer to the panel and the global M/N loading on the joint. In the model illustrated in Figure 1, the panel is contrariwise modelled by one spring, and so by one “equivalent” force acting on an equivalent height named  $z$ . No exact definition of  $z$  is known and, besides that, it changes at each loading step for all the here-above mentioned reasons.

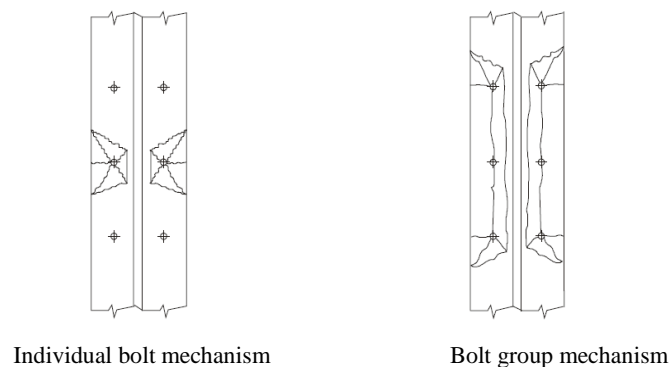


Fig. 3 - Example of possible plastic mechanisms in a column flange or an end-plate

A spring-model able to accommodate these three features is under development at Liege University and will allow an almost “exact” prediction of the joint properties. But in the

present paper, the focus is made on the development of an analytical assembly procedure, but with would respect all the physical requirements in terms of group effects and components interaction. The scope is so limited to the response of the “connections”. An extension to “joints”, i.e. including the “web panel in shear” component, is however proposed in [4].

In Section 3, the response of connections involving ductile components will first be addressed. Then, in Section 4, the influence of the presence of non-ductile components will be pointed out. In Section 5, the assembly procedure will be validated comparing the obtained analytical predictions to experimental results from tests performed on steel and steel-concrete composite connections. Finally, in Chapter 6, the present Eurocode 3 recommendations on M-N interaction will be commented.

### 3 DUCTILE CONNECTION RESISTANCE INTERACTION DIAGRAM

#### 3.1 Definition

The interaction diagram of a ductile connection subjected to M and N results in a plastic resistance surface; the resistance of the connection is ensured if the applied moment and axial force define a couple of values which remains inside the interaction surface.

#### 3.2 Conventions

The plasticity surface is defined in a general way here below for a connection made of a bolted end-plate with  $N_b$  rows of bolts through which only tensile loads may potentially be transferred and 2 zones of compression conventionally located [4] at mid-thickness of the upper and lower flanges of the connected beam (respectively noted “upper” or “up” and “lower” or “lo” and constituted, as seen in Figure 2, of two components: column web in compression (CWC) and beam flange and web in compression (BFC). This results in a total of rows equal to  $N_b+2 = n$  in which internal forces may appear. By convention, a compression force is assumed to be negative, or equal to zero while a tension force is positive or equal to zero. All the rows are numbered from 1 to  $n$  by starting from the row at the top. For an extended end-plate connection with one external bolt row, for instance, the compression row “up” is the row  $n^\circ 2$ , while it is the row  $n^\circ 1$  for a flush end-plate connection.

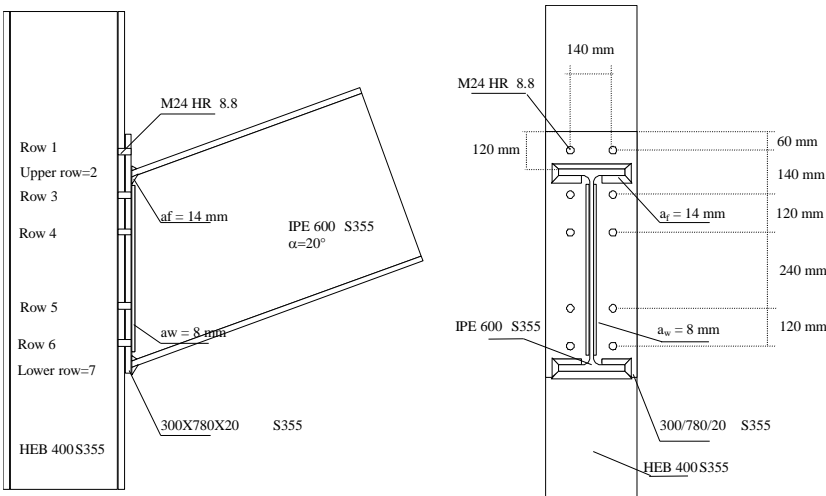


Fig. 4 – Bolted joint with numbering of force transfer rows

This is illustrated in Figure 4 for a joint with an extended end-plate connection including 5 ( $=N_b$ ) bolt rows. The kinematics of the problem is such that, for instance:

- the force in row n° 2 (“upper”) is equal to zero when the forces in rows n° 1 and 3 are different from zero;
- the bolt group mechanism noted [1,4] will only involve rows in tension, n° 1, 3 and 4.

### 3.3 Assumptions and bases for the definition of the interaction diagram

The behaviour of each joint component, and therefore of all the load transfer rows, is assumed to have an infinite ductility. Accordingly, a plastic redistribution of the internal forces within the joint carried out on the basis of the so-called static theorem to which it is here referred [1] may be contemplated. In other words, for M-N combinations, a full plastic distribution of internal forces in equilibrium with the externally applied forces will be defined and the related load factor level will be computed.

How to achieve this goal is extensively described in [4] and reported in Section 3.6. But before, the equilibrium and resistance criteria to fulfil are expressed in the two following sections.

### 3.4 Equations of equilibrium for the connection and eccentricity of the load

Based on the static theorem, it is possible to predict the resistance of a connection at failure by expressing the equilibrium between the external applied forces and the internal forces. When a connection is subjected to M and N, the equations of equilibrium write:

$$\begin{aligned} M &= \sum_{i=1}^n h_i \cdot F_i \\ N &= \sum_{i=1}^n F_i \end{aligned} \quad (2)$$

where  $F_i$  designates the force in row  $i$  and  $h_i$  the associated lever arm; this one is obtained computing the vertical distance between the considered row and the reference axis of the beam, i.e. the axis where M and N are considered to be applied ( $h_i$  is positive for the rows located above the reference axis).

The applied axial force and bending moment are linked through the concept of load eccentricity  $e$  as follows (the positive values of M and N are defined as indicated in Figure 2):

$$M = e \cdot N \quad (3)$$

### 3.5 Resistance criteria with due account of group effects

The resistance of a row is taken as equal to the resistance of the weakest component active in the considered row. To respect the static theorem, this resistance should never be exceeded. This looks easy when looking to the individual resistance of rows but is more difficult when group effects develop in the connections (see Section 2).

In the present study, any group of rows [m,p] for which group effects can develop is studied as an equivalent fictive row with an equivalent lever arm and a group resistance equal to that of the weakest component. Accordingly, the resistance criterion for each of the rows as part of the [m,p] group, for any component  $\alpha$ , can be written as follows:

$$\sum_{i=m}^p F_i \leq F_{mp}^{Rd \alpha} \quad m = 1, \dots, n \text{ and for each value of } m, p \text{ varies from } m \text{ to } n \quad (4)$$

where  $F_{mp}^{Rd \alpha}$  is the resistance of the [m,p] group for component  $\alpha$  computed according to Eurocode 3 Part 1-8. If  $m$  equals  $p$ ,  $F_{mp}^{Rd \alpha}$  becomes the individual resistance of the component  $\alpha$  included in row  $m$ . Such a resistance criterion may be derived for each of the constitutive row components and the final resistance of the group of rows [m,p], called  $F_{mp}^{Rd}$ , may be defined as the smallest of the  $F_{mp}^{Rd \alpha}$  values.

This criterion is illustrated in Figure 5 representing the application of this criterion for a connection with two bolt rows; the application of the criterion for a connection with three bolt rows, noted 1, 2 and 3, is presented in Figure 6. More globally, these figures cover cases met in any connections with  $n$  rows for which group effects could develop in two or three successive rows.

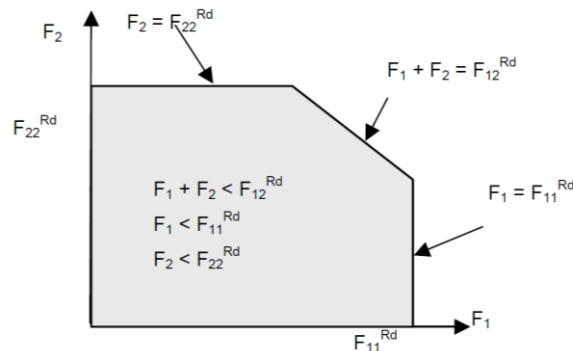


Fig. 5 - Interaction between two bolt rows

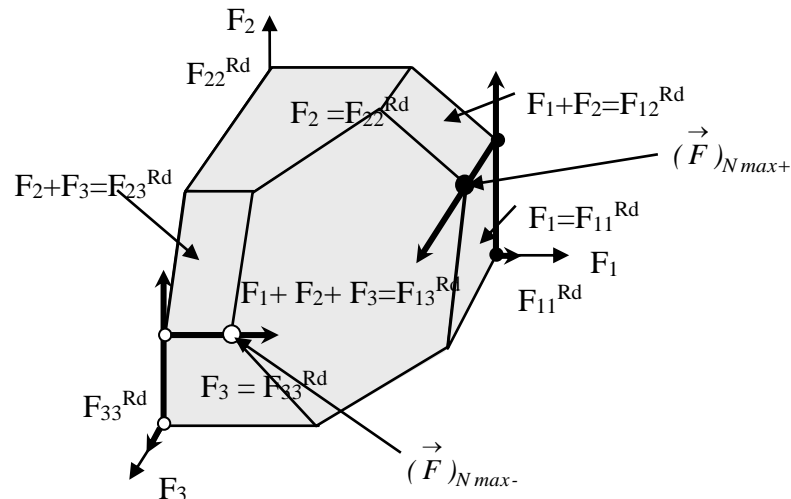


Fig. 6 - Interaction between three bolt rows and definition of  $F_j^{Rd}$  - Possible group effects between three bolt rows and successive steps for the evaluation of a connection resistance (black and white dots respectively).

### 3.6 Definition of the failure criterion for the whole connection

The resistance M-N interaction curve is obtained using the failure criterion provided by Equation 5; this one is explained in details in this section.

In this equation, the value of k is varying from 1 to n where n represents the total number of rows. k designates the number of the particular row where the plastic neutral axis is assumed to be located for the computation of different points of the M-N resistant curve (between these points of the M-N resistant curve, the plastic neutral axis is passing from one row to the following one); accordingly, by varying the value of k, different distributions of resistant forces amongst the rows are obtained (respecting the static theorem) and so, different M-N couples are obtained. Knowing that for each position of plastic neutral axis, two distributions of resistant forces can be obtained (one assuming that the part above the plastic neutral axis is under compression and the part below is under tension and one assuming the reverse situation), “2k” M-N couples are obtained using Equation 5. This equation is defined so as to obtain the maximum resistance in bending by adopting an optimised distribution of the internal loads amongst the activated rows, taking into account the possible group effects as explained here below.

$$M = h_k \cdot N + \sum_{i=1}^n (h_i - h_k) \cdot F_i^c \quad (5)$$

In this expression, two different resistances  $F_i^c$  can be attributed to row i ( $F_i^{Rd+}$  and  $F_i^{Rd-}$ ) with the objective to maximize the absolute value of the bending resistance by maximising the loads in the rows which are the most distant from the row “k”. This is illustrated for a connection with two bolts rows in Figure 7. Let assume that, in this connection, the resistance of the two bolt rows in tension is governed by the component “End-plate in bending” and that the corresponding group resistance is equal to 100 kN and is smaller than the sum of the individual resistances of the two bolt rows ( $2 * 60 \text{ kN} = 120 \text{ kN}$ ). In Figure 7, two situations are considered in which the number of the row k is respectively considered as equal to 1 and 4. The distribution of the tensile loads in the two bolt rows, for  $k = 1$  and for  $k = 4$ , is illustrated in Figure 7. If k is equal to 4 and a positive moment is applied to the connection, it means that the resistance of the upper bolt row  $F_2^{Rd+}$  is equal to 60 kN and the one of the lower bolt row  $F_3^{Rd+}$  is equal to 40 kN ( $= 100 \text{ kN} - 60 \text{ kN}$ ) while, if  $k = 1$  and a negative moment is applied to the connection, the resistance of the upper bolt row  $F_2^{Rd-}$  is equal to 40 kN and the one of the lower bolt row is equal to 60 kN. Such a procedure is illustrated in Figure 6 for a joint in which three bolt rows are possibly concerned by group effects. The black dots show the successive steps to estimate  $F_i^{Rd+}$  respecting the group resistances while the white ones show the steps to estimate  $F_i^{Rd-}$ . Accordingly,  $F_i^{Rd+}$  and  $F_i^{Rd-}$  can be defined as the maximum (or minimum in case of negative values) resistance of row i under positive and negative moments respectively considering the group effects and maximising the resistant moment. More details about the definition of this failure criterion can be obtained in reference [4] that can be afforded to any interested reader.

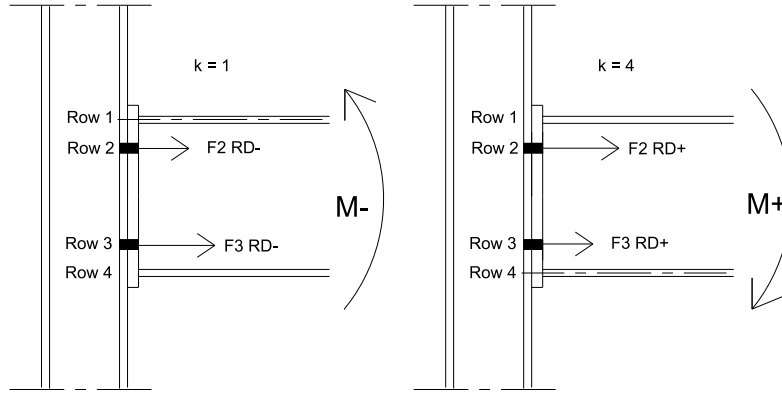


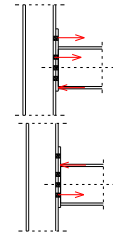
Fig. 7 – Examples of distribution of resistant forces amongst the rows in tension on a connection with two bolt rows

This results in the following definition of the M-N resistance interaction diagram:

*The interaction resistance criterion between the bending moment (M) and the axial force (N) at failure is provided by a set of 2 n parallel straight line segments; the slope of each of the 2 n parallel segments is equal to the value of the lever arm ( $h_k$ ) and along these segments, the force ( $F_k$ ) varies between 0 at one end and the maximum resistance row resistance at the other end.*

The application of Equation 5 may be written with more details as follows:

$$\begin{aligned}
 M &= h_k \cdot N + \sum_{i=1}^n (h_i - h_k) \cdot F_i^c \\
 \text{either } \left. \begin{aligned} F_i^c &= \max(F_i^{Rd+}; 0) \text{ if } i < k \\ F_i^c &= \min(F_i^{Rd+}; 0) \text{ if } i > k \end{aligned} \right\} & \text{tension in the rows at the top (M}^+) \\
 \text{or } \left. \begin{aligned} F_i^c &= \min(F_i^{Rd-}; 0) \text{ if } i < k \\ F_i^c &= \max(F_i^{Rd-}; 0) \text{ if } i > k \end{aligned} \right\} & \text{tension in the rows at the bottom (M}^-) \\
 \text{with } F_i^{Rd+} &= \min(F_{mi}^{Rd} - \sum_{\substack{j=m \\ i \neq up, lo}}^{i-1} F_j^{Rd+}, m = 1, \dots, i) \text{ for } i < k \text{ and } F_i^{Rd+} = F_i^{Rd} \text{ for } i = up, lo > k \\
 F_i^{Rd-} &= \min(F_{im}^{Rd} - \sum_{\substack{j=i+1 \\ i \neq up, lo}}^m F_j^{Rd-}, m = i, \dots, n) \text{ for } i > k \text{ and } F_i^{Rd-} = F_i^{Rd} \text{ for } i = up, lo < k
 \end{aligned}
 \tag{6}$$



### 3.7 Ductile resistance of the connection and stress interaction between components phenomenon

As expressed in Section 2, for connections, Part 1.8 of Eurocode 3 considers that stress interaction phenomena can affect the resistances of the two following column's components:

- column web in compression (CWC);
- column web in tension (CWT);

The resistance of these components is first affected by a reduction factor depending on the transformation factor called  $\beta$  equal defined in Eurocode Part 1-8 as the ratio between the

shear force acting in the CWS component and the load-introduction force transmitted to the column by the CWC or CWT components. It leads to the reduction by a  $\beta$ -dependent coefficient  $\omega$  of the CWC and CWT resistances in Part 1.8 of Eurocode 3. The definition of  $\beta$  is illustrated in Figure 8 for a single-sided and a double-sided joint configuration with welded connections.

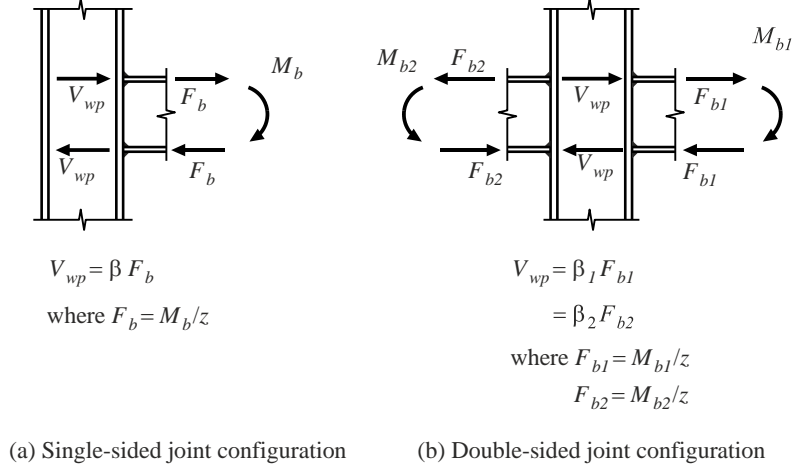


Fig. 8 - Illustration of the definition of the transformation factor  $\beta$

The shear force  $V_{wp}$  in the column web panel component (CWS) resulting from equilibrium equations writes (see Figure 9):

$$V_{wp} = (M_{b1} - M_{b2}) / z - (V_{c1} - V_{c2}) / 2 \tag{7}$$

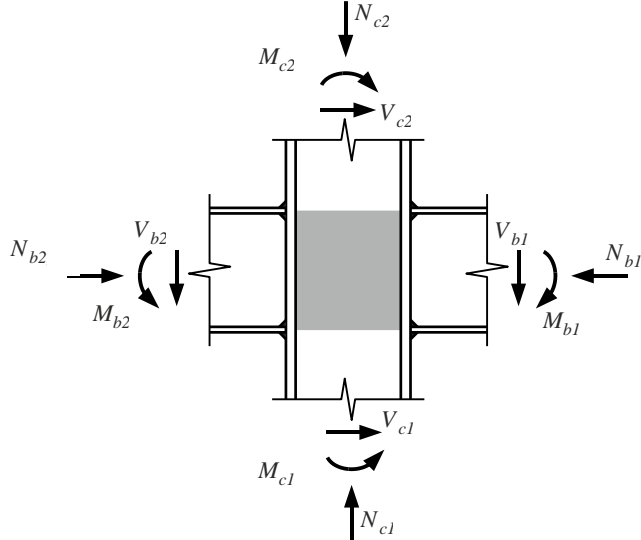
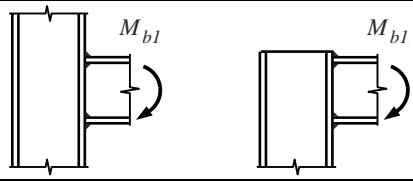
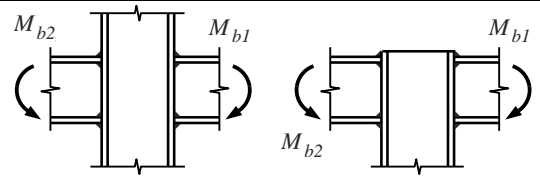


Fig. 9 - Forces applied at the periphery of a column web panel

In classical situations in which the column lengths is significantly higher than the column web panel height, Eurocode Part 1-8 suggest a simplification in the form of approximate values of the transformation factor  $\beta$ , see Table 1.

Table 1: Approximate values for the transformation parameter  $\beta$

Type of joint configuration	Action	Value
	$M_{b1}$	$\beta \approx 1$
	$M_{b1} = M_{b2}$	$\beta = 0$ *)
	$M_{b1} / M_{b2} > 0$	$\beta \approx 1$
	$M_{b1} / M_{b2} < 0$	$\beta \approx 2$
	$M_{b1} + M_{b2} = 0$	$\beta \approx 2$
*) In this case the value of $\beta$ is the exact value rather than an approximation		

In addition, the resistance of the CWC component may be influenced by the longitudinal stress associated to bending moment and axial force in the column ( $k_{wc}$  coefficient in Part 1.8 of Eurocode 3). Generally, the  $k_{wc}$  coefficient is equal to 1,0 and no reduction is required. Therefore, it can be omitted in preliminary calculations, when the longitudinal stress is unknown; this assumption has however to be checked later in the design process.

For any eccentricity (ratio between M and N), these factors are different and may play a role or not. For example, if the actual “corrected” resistance of the CWC component remains larger than the one corresponding to the BFC (beam flange and web in compression) component one, the stress interaction in the CWC component does not have any influence on the M-N interaction diagram. In the same way, if EPB or BWT (beam web in tension) components determine the resistances of the bolt rows in tension, stress interaction in component CWT does not play any role in the derivation of the M-N interaction diagram.

On the other way, if component influenced by the stress interaction determine the resistances  $F^{Rd+}$  and  $F^{Rd-}$ , it should be clear that these values may vary. As for joints subjected to moment only, an exact calculation requires an iterative procedure as the level of stress interaction is depending of the level of the forces. Furthermore the M-N interaction diagram is no more constituted of 2n parallel segments, the resistance of one or several rows varying continuously according to the loading. Practically, this iterative procedure is limited to one or two iterations and could be undertaken in a first approximation only for the limiting points of the segments of the former interaction diagram as it is shown on an example in Section 3.8.

### 3.8 Definition of the ductile resistance of the connection of the example

Fig. 10 shows the M-N interaction resistance diagram computed for the connection described in Figure 4.

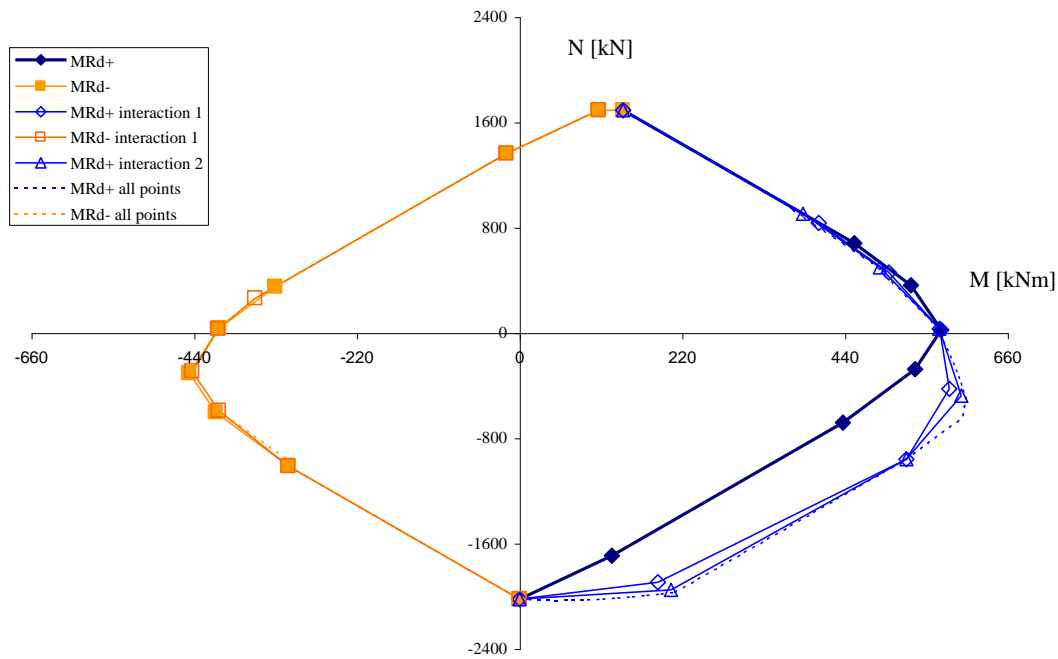


Fig. 10 - Interaction diagrams of the connection shown in Figure 4 and influence of the stress interaction phenomena

For such a single-sided joint configuration, Eurocode 3 Part 1-8 recommends safely to consider that the coefficient  $\beta$ , which influences the resistance of the CWT and CWC components, equals 1,0 but for joints subjected to bending moment only. For other loading situations (in other words, under M and N), a specific value of  $\beta$  should be selected to account for the relevant level of shear forces in the column web panel. As an example, for a joint in compression or tension only,  $\beta$  decreases and can almost reach a zero value in some cases. To consider that  $\beta$  is equal to 1,0 whatever is the loading situation may initially appear as a safe (even sometimes much too safe) assumption. This has been assumed, in Figure 7, for the “ $M_{Rd+}$ ” and “ $M_{Rd-}$ ” diagrams which therefore form the ductile M-N resistance interaction curve obtained, through Equation 5, by assuming a constant reduction of resistance for the CWT and CWC components. The signs (+) and (-) refers to zones of the curve where positive and negative bending moments are respectively predominant.

In order to derive more precise interaction curves duly accounting for the actual interaction level through an exact value of  $\beta$ , an iterative procedure has to be initiated. The “ $M_{Rd}$  interaction 1” curves and the “ $M_{Rd}$  interaction 2” curves are so obtained, starting from the “ $M_{Rd+}$ ” and “ $M_{Rd-}$ ” ones, by progressively refining the value of  $\beta$ . Two iterations are more than enough to reach convergence, as seen on Figure 6. In this process, constant values of  $\beta$  are considered on each segment of the interaction curves. In most of the loading situations, higher resistances are obtained than those reported in the “ $M_{Rd+}$ ” and “ $M_{Rd-}$ ” curves, as  $\beta$  is there smaller than 1,0. In the “ $M_+ - N_+$ ” quarter, the reverse is contemplated for few points in which  $\beta$  is there larger than 1,0.

Finally, “ $M_{Rd}$  all points” curves present the results obtained by evaluating continuously the stress interaction, i.e. specifically at each of its points. This diagram is very similar to the one calculated only with a few points, except locally in the “ $M_{Rd+}$ ” part of the diagram. One

additional point could however be calculated when required so as to ensure more accurate results.

To build the complete M-N curve allows the designer to check the joint for the different loading situations resulting from the various combinations of load cases imposed by the norms, but can appear as tedious when only one single load case has to be practically consider. In [4], practical application methods are proposed which permit a direct estimation of the connection resistance for a specific value of the load eccentricity; this aspect is not addressed here.

## 4 NON-DUCTILE CONNECTION RESISTANCE INTERACTION DIAGRAM

### 4.1 Non-ductile components

The ductility of some components is sometimes not sufficient to enable the full plastic redistribution of the internal forces assumed in the method presented in Section 3. During the loading process, when one fragile component reaches its capacity of deformation, any additional increase of the loading causes the brittle failure of that component and consequently the brittle failure of the whole connection.

Part 1.8 of Eurocode 3 considers explicitly bolts in tension (BT) and welds as brittle components. Besides that it assumes that the capacity of deformation of a plated component (end-plate in bending or column flange in bending) is sufficient to allow for complete internal redistribution of forces in the connection if its design resistance  $F^{Rd}$  is lower or equal to 95% of that of the bolts in tension.

Moreover, the flange and web of the beam in compression (BFC) may also be considered as a non-ductile component when the beam profile becomes slender and its resistance defined by buckling phenomena (class 4 sections). The same conclusions apply to column webs in compression (CWC).

The non-ductile behaviour of these components may lead to a reduction of the connection resistance capacity. The way on how to adapt the M-N interaction curve accordingly is explained in the next paragraph.

### 4.2 Analytical calculation of the non-ductile resistance of the connection

The resistance of a connection is here assumed to be reached once the deformation of a non-ductile component is equal to its deformation capacity.

In Figure 2, and according to the so-called Bernoulli principle (a plane section remains plane), the beam end-section close to the connection remains un-deformed. This may be expressed through Equation (8) where  $\Delta$  and  $\varphi$  are the displacements corresponding to the zero-lever arm ( $h_{\Delta}=0$ ) and the rotation of the connection (if the panel zone is disregarded, what is the case here). The knowledge of the displacement of two rows is then sufficient to define the entire deformation of the joint.

$$\Delta_i = \Delta + h_i \cdot \varphi \quad (8)$$

Nevertheless, when a component of a row  $k$  reaches its maximum capacity of deformation, the only row whose deformation is known is the one of row  $k$  ( $\Delta_k^{\text{Rd}}$ ). The deformation in another row is needed to define the deformation of the connection. The easiest way to define the non- ductile behaviour due to row  $k$  is then to assume a given deformation of another bolt row or to assume a given position of the zero displacement point ( $h_0$ , defined by Equation 9).

$$\Delta_0 = 0 = \Delta + h_0 \cdot \varphi \Rightarrow h_0 = -\frac{\Delta}{\varphi} \quad (9)$$

$$\Delta_i = (h_i - h_0) \cdot \varphi \quad \forall i$$

By varying the value of  $h_0$  from  $-\infty$  to  $+\infty$ , the all possible states of deformation of the connection corresponding to the limited capacity of deformation of row  $k$  are obtained.

The proposed method comprises then the following steps for each row  $k$  presenting a non-ductile behaviour:

- calculation of the deformation capacity  $\Delta_k^{\text{Rd}}$  of row  $k$  presenting a non-ductile behaviour and selection of one value of zero point displacement  $h_0$ ;
- calculation of the displacement  $\Delta_i$  for all rows and definition of the internal force  $F_i$  in these rows using the behavioural law characterising these rows (relation between  $F_i$  and  $\Delta_i$ );
- evaluation of the axial and bending forces corresponding to these internal forces;
- re-application of the procedure until the whole domain of values of  $h_0$  has been examined.

That method should also take into account the stress interaction. This is only possible with the help of an iterative procedure, the level of stress interaction depending on the level of forces, unknown at the beginning of the calculation. Nevertheless, as the state of displacement is independent of that stress interaction, that calculation is rather simple and generally requests only two iterations as explained above.

### 4.3 Definition of the non-ductile resistance of the example

For the example, let assume that the resistance of two bolt rows (rows 3 and 6) in the connection reported in Figure 4 corresponds to non-ductile failure modes (BT). The M-N interaction diagram defined previously assuming a ductile behaviour for all rows should then be corrected. The procedure explained above is so applied, what leads, in Figure 11, to corrections (i.e. reductions) of the resistances in two zones of the M-N interaction curve.

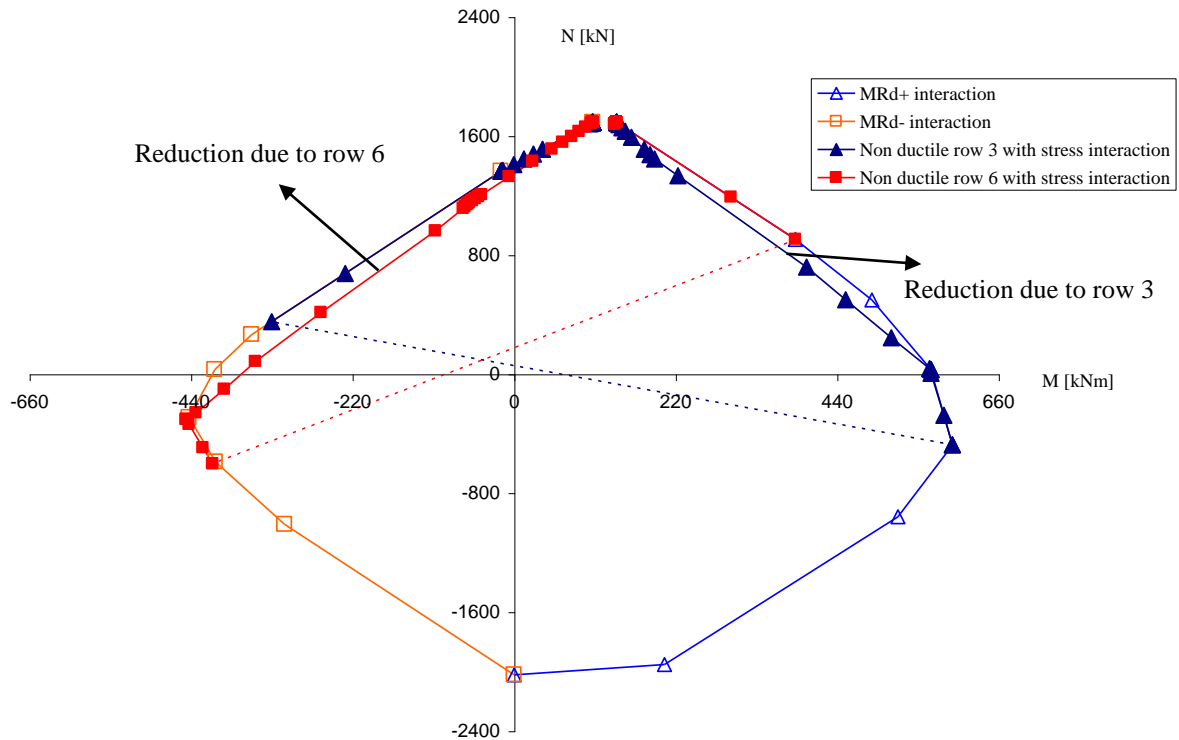


Fig. 11 - M-N diagram of the studied connection considering a non-ductile behaviour of rows 3 and 6 (with stress interaction)

## 5 COMPARISON WITH LABORATORY TESTS

### 5.1 Definition of the experimental resistance

Tests on joints or connections are generally performed until failure. While failure does not occur in the elastic range, failure is reached once the deformation of one or more components is in the plastic range. The importance of that post-elastic behaviour depends on the ductility of the component(s) that fail. If a complete plastic redistribution of the internal forces develops, the so-called plastic resistance is reached.

Once the plastic resistance is exceeded, strain-hardening may develop as long as the ultimate deformability of one of the components is not reached. This is illustrated in Figure 10 for a beam-splice bolted connection (test NN1000) performed at the University of Prague [9] (see Figure 12). The coordinate of the point at the intersection of the two lines, one corresponding to the elastic stiffness and one to the strain-hardening stiffness, conventionally represents the experimental plastic resistance of the connection. This value is reported as  $M_{Rd}$  in Figure 13.

In the comparisons presented below, the experimental value will be considered as the maximum level of resistance reported during the test, but never exceeding  $M_{Rd}$ , so as to be in full compliance with the definition of the resistances predicted by EC3 Part 1-8 and by the procedure presented in Sections 3 and 4 of the present paper. In the comparative graphs, the EC3 Part 1-8 “M-N” interaction diagram will be reported too. Conclusions about the level of accuracy will be discussed in Section 6.



Fig. 12 - Flush end-plate joint NN1000 (Prague) at collapse, yielding of the end-plate in bending (EPB) and of the beam flange and web in compression (BFC) [9]

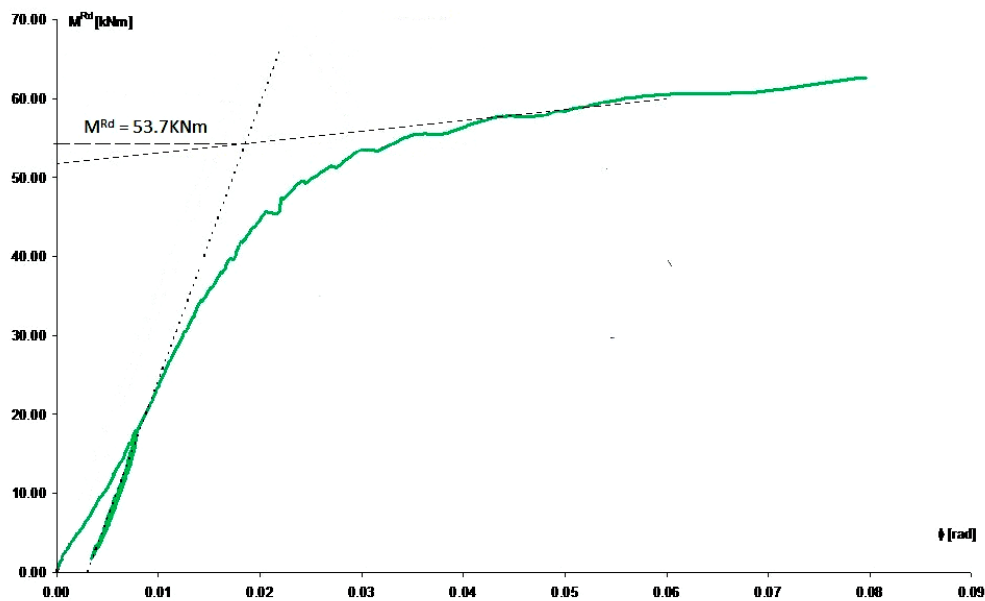


Fig. 13 - moment-rotation curve of the flush end-plate joint NN1000 (Prague)  
Definition of the design resistance [9]

## 5.2 Steel joints tested in Prague

Two types of joints have been tested in Prague [9]:

- Beam splices (IPE200) - flush end-plate and 4 bolts M12 (3 tests)
- Beam-to-column (IPE180) joints - extended end-plate and 6 bolts M12 (2 tests)

All joints are considered here as long as the column web panel is not governing the failure of the beam-to-column joints.

Loading eccentricity remains unchanged during a test but differs from one test to the other.

The analytical interaction diagram and the results of the tests for flush and extended end-plate joints are reported respectively in Figures 14 and 15 and in Tables 2 and 3. The results according to Part 1.8 of EC3 are also reported in the figures.

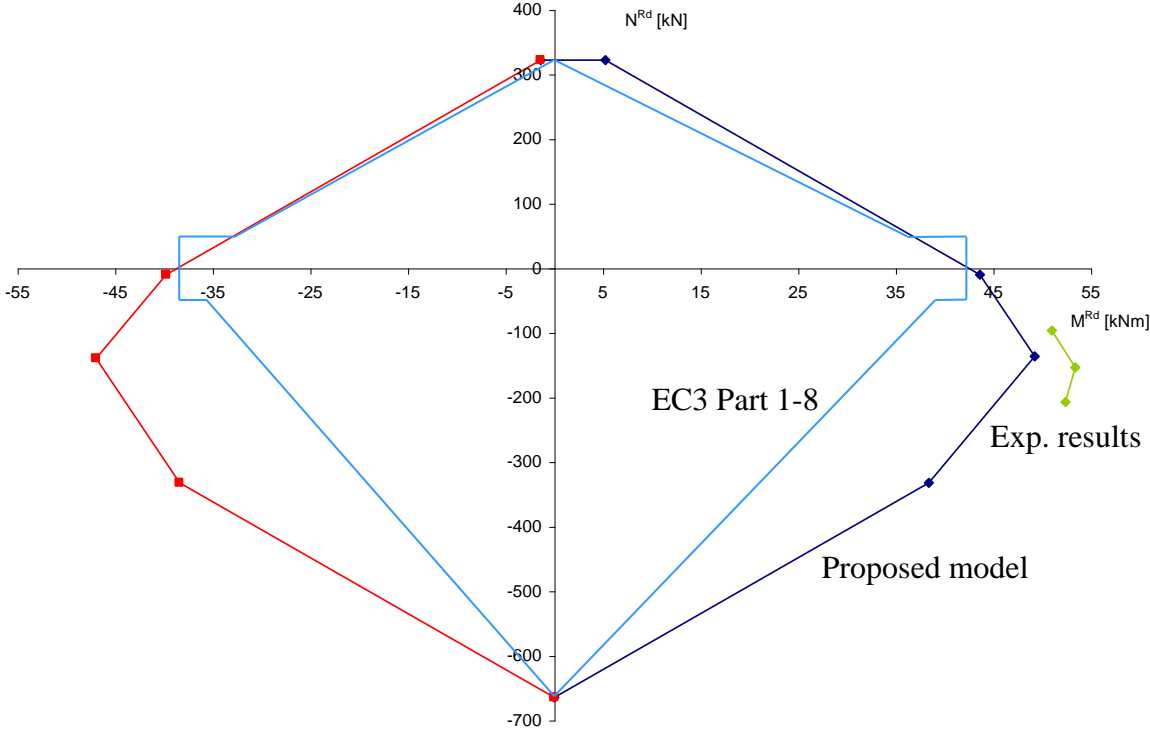


Fig. 14 - Interaction diagram for flush end-plate joints tested in Prague (NN joints), tests and analytical method

Table 2: Comparison tests/analytical method for flush end-plate joints tested in Prague (NN joints)

Test		Resistance [kNm]		
Name	e [mm]	Test	Analytical	$\Delta$ [%]
NN750	-252.97	52.4	45.57	-13
NN1000	-347.41	53.7	48.96	-8.3
NN1500	-529.22	51	47.15	-7.5

For the flush end-plate joints NN, the agreement between analytical results and tests is rather good and moreover the three test points indicate a trend in the interaction that is also observed by the analytical method (different failure modes). The average difference between tests and the analytical method is less than 10%.

For extended end-plates joints SN, the accordance between analytical results and the two test results is also rather good. Nevertheless, the limited number and the range of the tested eccentricity do not allow confirming that the stress interaction in the column web in compression plays a role such as indicated by the analytical calculations.

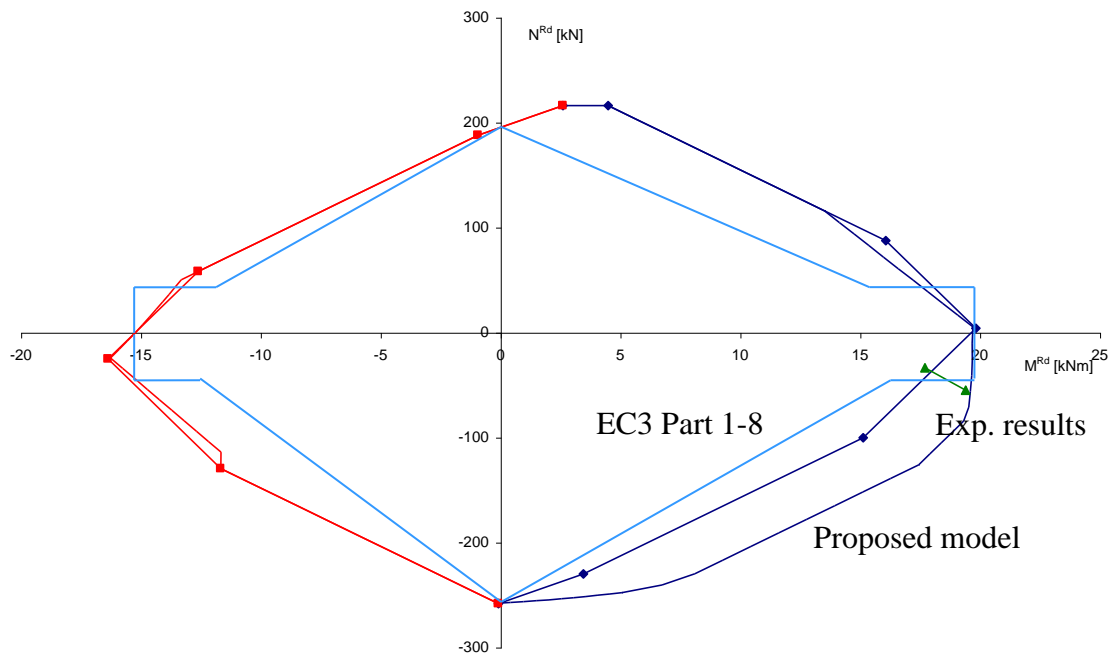


Fig. 15 - Interaction diagram for extended end-plate joints tested in Prague (SN joints), tests and analytical method

Table 3: Comparison tests/analytical method for extended end-plate joints tested in Prague (SN joints)

Test		Resistance [kNm]		
Name	E [mm]	Test	Analytical	$\Delta$ [%]
SN1000	-353.46	19.4	19.6	1.0
SN1500	-527.69	17.7	19.66	11.1

### 5.3 Steel-concrete composite joints tested in Stuttgart

The design procedures provided in Eurocode 3 for steel joints are extended in Eurocode 4 [2] to steel-concrete composite joints exposed to hogging moments through the introduction of appropriate extra components rules. One of the only specificities lies in the fact that the “longitudinal steel reinforcement in tension” will be treated as a “bolt-row in tension” with specific resistance and stiffness tension properties. However, no information is provided in Eurocode 4 on the prediction of the component “slab in compression” which may be activated under axial compression forces or sagging bending moments. In [5] and [12], specific design rules are proposed, detailed and validated by the first author and these ones are considered in the present study.

The validity of the proposed procedure presented in the previous sections is here checked through comparisons to experimental results obtained from tests performed at the University of Stuttgart in the framework of an RFCS project [10]. The five tests relate to a single joint

configuration but are achieved so as to cover the “M-N” interaction domain, including sagging and hogging moments, but also axial tension forces.

The comparison between the analytical predictions and the experimental results is reported in Figure 13. The analytical predictions have been obtained using the actual mechanical properties of the materials; the details of all the calculations required to obtain the analytical predictions are provided in [5].

On this figure, two analytical curves are provided:

- one named “plastic resistance curve” which is calculated using the actual elastic strengths of the materials and;
- one named “ultimate resistance curve” which is calculated using the actual ultimate strengths of the materials.

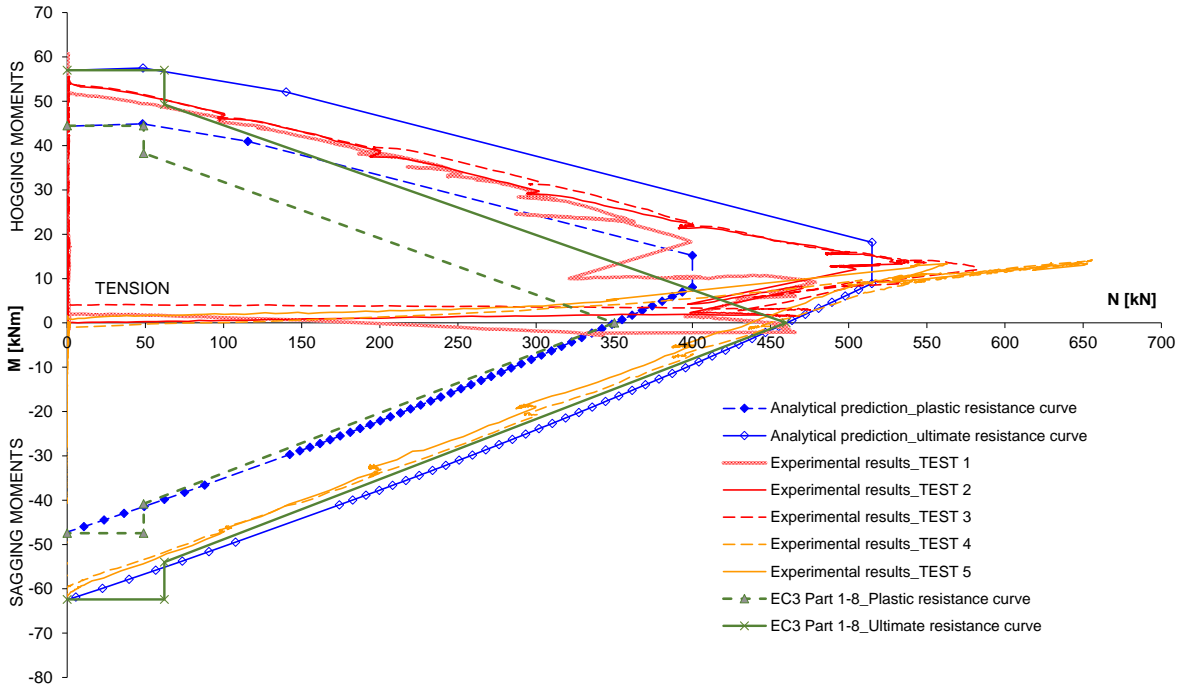


Fig. 16 - Comparison between the predicted analytical curves and the experimental ones

Looking to Figure 16, it can be observed that the predicted analytical curves are in very good agreement with the experimental ones. Indeed, it appears that the experimental curves are above the plastic analytical resistance curves but below the ultimate analytical resistance curves; this is corresponding to the sequence of loading followed during the experimental tests as justified here below.

In the zone of hogging moments, the experimental curves are close to the analytically predicted ultimate curve for limited values of tension forces; this is line with the testing procedure as the experimental tests started first with the application of a bending moment which was increased up to a value close to the ultimate bending resistance of the joint before the application of the tension forces. Then, when the tension force is increased, the experimental curves diverge from the ultimate analytical curve before coming back closer to the ultimate analytical curve (except for TEST 1). This can be justified by the fact that different joint components are activated to pass from the ultimate bending resistance to the

ultimate tensile resistance; indeed, the component associated to the ultimate bending resistance is the “beam flange in compression” while the one related to the ultimate tensile resistance is the “column flange in bending”.

In the sagging moment zone, a different behaviour is observed; indeed, as can be seen in Figure 16, the experimental curves are remaining close to the ultimate analytical curve from pure bending to the ultimate tensile resistance. Once more, it is in line with the component activated at failure which is here the same from pure bending to pure tension, i.e. the “column flange in bending” component.

#### **5.4 Steel-concrete composite joints under elevated temperature tested in Coimbra**

In the framework of a European RFCS project called ROBUSTFIRE, the response of steel and steel-concrete composite car park structures subjected to a localised fire resulting in a column loss was studied. Under the considered scenario, it has been demonstrated that the structural beam-to-column joints play an important role in the global structural behaviour. Indeed, these joints, mainly loaded in bending at room temperature, may be exposed to elevated temperatures and to combined axial load “N” and bending moment “M”.

Experimental tests on composite joints at high temperature have been performed at this occasion at the University of Coimbra and “M-N” resistance interaction curves have been obtained. In [11], the interested reader will find details about the experiments but will also appreciate the way on how the component approach and design model proposed in the present paper have been used to predict accurately the M-N behaviour joints at high temperature.

#### **5.5 Conclusions of the comparison with laboratory tests**

The accordance between the tests results and the proposed analytical method is fully acceptable since differences remain rather limited. Besides that, some more specific aspects tend to increase the confidence that one could have in the model:

- The global shape of the experimental “M-N” interaction curves is pretty well predicted by the analytical methods as seen through the comparisons on composite joints.
- Many different failure types are observed for the different tests with the same accuracy in the comparisons.
- The resistance of one test configuration (SN) is influenced by stress interaction phenomena, but a similar level of accuracy than for other tests is analytically obtained.

### **6 EVALUATION OF THE EUROCODE 3 MODEL FOR M-N INTERACTION**

As seen in Figure 1, the Eurocode “M-N” interaction resistant curve is a quadrilateral whose corners correspond to resistances under pure axial forces and pure bending moments. A zone of “no-interaction” is then superimposed which corresponds to 5% of the plastic axial resistance of the connected beam.

A first conclusion which may be easily drawn concerns the “non-interaction” domain, which appears as clearly inappropriate: it is seen to be sometimes safe, sometimes unsafe, but for sure never reflecting the actual physical trends. To maintain it further in Eurocode 3 Part 1-8 looks therefore quite questionable.

As far as the linear interaction model is now concerned, its safe character may be contemplated, as well as its accuracy in some “M-N” interaction domains. The underestimation of the actual connection resistance to which it leads in many cases reduces however its economic interest.

An improvement of the model could consist in keeping a “M-N” quadrilateral model, but in which the four corners to the maximum resistances of the connection in hogging/sagging bending moments (with a possible axial force) and in compression/tension forces (with a possible bending moment). Obviously, the norm should practically explain how to derive these four resistances.

## 7 CONCLUSIONS

Analytical procedures for the prediction of the design resistance of steel bolted connections and steel-concrete composite connections subjected to combined bending moment and axial force are proposed in the present paper. These ones are fully in agreement with the principles contained in Part 1.8 of Eurocode 3 and in Eurocode 4.

These procedures differ from other ones which have been already proposed by other authors by their ability to cover so-called group-effects and accommodate ductile as well non-ductile failure modes.

Series of tests on steel and composite bolted joints under bending and axial forces have been introduced and their resistance compared with the one provided by the proposed analytical methods. The agreement between tests and analytical methods may be judged fine with an average difference between tests and predictions of less than 10%.

The adequacy of the Eurocode 3 Part 1-8 recommendations in terms of M-N interaction are critically analysed and their limitation and potential under- and overestimation of the actual resistances are pointed out. Suggestions for improvement are finally made.

In a forthcoming publication, the authors intend to show how the analytical developments contained in the present paper could be extended to joints, including column web panels in shear.

## REFERENCES

- [1] *EN 1993-1-8 Eurocode 3: Design of steel structures - Part 1.8: Design of joints*, CEN, Brussels, 2005.

- [2] *EN 1994-1-1 Eurocode 4: Design of composite steel and concrete structures: Part 1.1: General rules and rules for buildings*, CEN, Brussels, 2004.
- [3] Jaspert J.-P., K. Weynand K.: *Design of joints in steel and composite structures*, ECCS Eurocode Design Manual, Wiley, Ernst & Sohn, 2016.
- [4] Cerfontaine F.: *Etude de l'interaction entre moment de flexion et effort normal dans les assemblages boulonnés*. PhD Thesis. University of Liège, 2003.
- [5] Demonceau, J.-F.: *Steel and composite building frames: sway response under conventional loading and development of membrane effects in beams further to an exceptional action*, PhD dissertation, University of Liège, 2008.
- [6] Del Savio A.A., Nethercot D.A., Vellasco P.C.G.S., Andrade S.A.L. and Martha L.F.: *Generalised component-based model for beam-to-column connections including axial versus moment interaction*. Journal of Constructional Steel Research, 65(2009), pp. 1876-1895.
- [7] Liu Y., Malaga-Chuquitaype C. and Elghazouli A.: *Response of beam-to-column angle connections subjected to combined flexure and axial loading*. Proceedings of the Tubular Structures XIV Conference, Taylor & Francis Group, London, edited by Gardner, 2012, pp. 133-139
- [8] Urbonas K. and Daniunas A.: *Component method extension to steel beam-to-column knee joints under bending and axial forces*. Journal of Civil Engineering and Management, Vol. XI, N° 3, 2005, pp. 217-224.
- [9] Svarc M. and Wald F.: *Experiments with end-plates joints loaded by moments and normal forces*, Acta Polytechnica, Prague, September 2001.
- [10] Kuhlmann U., Rölle L., Jaspert J.P., Demonceau J.F., Vassart O., Weynand K., Ziller C., Busse E., Lendering M., Zandonini R. & Baldassino N.: *Robust structures by joint ductility*, Final Report of a RFCS project, Science Research Development, European Commission, 2008.
- [11] Demonceau J.F. Haremza C., Jaspert J.P., Santiago A. and Simoes da Silva L.: *Composite joints under M-N at elevated temperatures - Experimental investigations and analytical model*. Proceeding of the Composite Construction VII conference, Palm Cove, Australia, July 2013, pp. 387.
- [12] Jaspert J.P. and Demonceau J.F. *Composite joints in robust building frames*. Proceeding of the 6<sup>th</sup> International Conference on Composite Construction in Steel and Concrete, Tabernash, USA, pp. 442-454, 2008.